

## **A Combined Transient and Brief Steady-State Technique for Measuring Hemispherical Total Emissivity of Electrical Conductors at High Temperatures: Application to Tantalum**

**T. Matsumoto<sup>1,2</sup> and A. Cezairliyan<sup>1,3</sup>**

*Received May 1, 1997*

---

A new method for measuring hemispherical total emissivity of electrically conducting materials at high temperatures (above 1500 K) using a feedback-controlled pulse-heating technique has been developed. The technique is based on rapid resistive self-heating of a solid cylindrical specimen in vacuum up to a preset high temperature in a short time (about 200 ms) and then keeping the specimen at that temperature under steady-state conditions for a brief period (about 500 ms) before switching off the current through the specimen. The specimen is maintained at constant temperature with a feedback control system which controls the current through the specimen. The computer-controlled feedback system operates a solid-state switch (composed of field-effect transistors). The sensing signal for the feedback is provided by a high-speed optical pyrometer. Hemispherical total emissivity is determined at the temperature plateau from the data on current through the specimen, the voltage drop across the middle portion of the specimen, and the specimen temperature using the steady-state heat balance equation based on the Stefan-Boltzmann law. The true temperature of the specimen is determined from the measured radiance temperature and the normal spectral emissivity; the latter is obtained from laser polarimetric measurements. The experimental quantities are measured and recorded every 0.2 ms with a 12-bit digital oscilloscope. To demonstrate the feasibility of the technique, experiments were conducted on a tantalum specimen in the temperature range 2000 to 2800 K. The results on hemispherical total emissivity are presented and are compared with the data given in the literature.

---

**KEY WORDS:** emissivity; hemispherical total emissivity; high temperatures; normal spectral emissivity; pulse heating; tantalum.

---

<sup>1</sup> Metallurgy Division, National Institute of Standards and Technology, Gaithersburg, Maryland 20899, U.S.A.

<sup>2</sup> Guest Scientist from the Measurement System Department, National Research Laboratory of Metrology, 1-1-4 Umezono, Tsukuba, Ibaraki 305, Japan.

<sup>3</sup> To whom correspondence should be addressed.

## 1. INTRODUCTION

Rapid resistive self-heating techniques have been developed and used extensively in our laboratory for measurements of selected thermophysical properties, including hemispherical total emissivity, of electrically conducting materials at high temperatures [1–4]. These techniques are based on rapid heating of the specimen from room temperature to the desired high temperature in less than 1 s by the passage of a high-current pulse through it. When the specimen reaches the preset temperature, the current is switched off, permitting the specimen to cool. Hemispherical total emissivity is determined from the data taken during the heating and the initial radiative cooling periods [1]. The required data include heating and cooling rates of the specimen, which can introduce significant uncertainties in the hemispherical total emissivity results since these rates are very sensitive to uncertainties in temperature measurements. A technique that does not require determination of heating and/or cooling rates is likely to yield more accurate values for hemispherical total emissivity.

In this paper, development of a new method for measuring hemispherical total emissivity of electrically conducting materials at high temperatures that does not require a knowledge of heating and/or cooling rates is presented. The technique is based on rapid resistive self-heating of a solid cylindrical specimen in vacuum up to a preset high temperature in a short time (about 200 ms) and then maintaining the specimen at that temperature under steady-state conditions for a brief period (about 500 ms) before switching off the current through the specimen. The specimen is maintained at a constant temperature with a feedback control system which controls the current through the specimen. The computer-controlled feedback system operates a solid-state switch [composed of field-effect transistors (FETs)]. The sensing signal for the feedback is provided by a high-speed optical pyrometer. Hemispherical total emissivity is determined at the temperature plateau from the data on current through the specimen, the voltage drop across the middle portion of the specimen, and the specimen temperature using the steady-state heat balance equation based on the Stefan–Boltzmann law. To demonstrate feasibility of the technique, experiments were conducted on a tantalum specimen in the temperature range 2000 to 2800 K. The results on hemispherical total emissivity are presented and compared with the data given in the literature.

It should be noted that the controllable switch is the key item that enabled development of the new technique. Until recently, the millisecond-resolution pulse-heating system in our laboratory utilized an electro-mechanical switch. This switch had a significant time delay between the trigger pulse and the actual switch closing, which prevented precise timing

of the current pulse. The mechanical switch was also not very reliable, as arcing between the contacts deteriorated its operation. To overcome the disadvantages of electromechanical switches, a solid-state switch for turning high currents on and off in millisecond-resolution pulse-heating experiments was developed by Matsumoto and Ono [5, 6]. The switch in the present study is an advanced version of the above solid-state switch. The present solid-state switch not only is capable of switching high currents (up to about 3000 A) on and off reliably in short times ( $<5$  ms) but also can rapidly adjust the current level from zero to the maximum rating in response to an applied control voltage.

## 2. PRINCIPLE OF THE TECHNIQUE

Figure 1 is a schematic diagram showing the temperature–time function for a specimen during an experiment conducted using the feedback control technique. The specimen undergoes an initial rapid pulse heating from an ambient temperature  $T_e$  to a high temperature  $T_s$ , followed by a brief steady-state period A at temperature  $T_s$ , before beginning to cool by thermal radiation.

The technique for measuring hemispherical total emissivity is based on the heat balance on the specimen when held at a preset high temperature  $T_s$ . Under steady-state conditions, the electrical power imparted to the specimen is equal to the power loss from the specimen. At temperatures above about 1500 K, heat loss from the “effective” (middle portion) specimen during the brief steady-state period (a fraction of a second) is primarily by

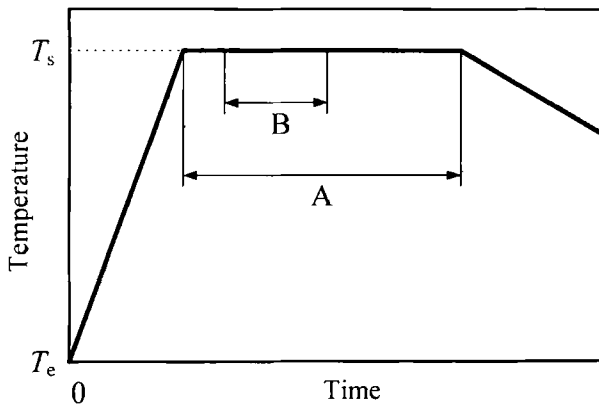


Fig. 1. Schematic diagram showing the temperature–time function for a specimen during an experiment conducted according to the feedback control technique.

thermal radiation. This is due to the fact that heat loss by axial conduction to the ends of the specimen is very small in comparison with heat loss by radiation. Based on the Stefan–Boltzmann law, the power balance on the effective specimen yields hemispherical total emissivity:

$$\varepsilon_{h,t} = \frac{EI}{A_s \sigma (T_s^4 - T_c^4)} \quad (1)$$

where  $E$  is the voltage drop across the effective specimen,  $I$  is the current through the specimen,  $T_s$  is the specimen temperature at the plateau,  $T_c$  is the temperature of the environment surrounding the specimen,  $A_s$  is the surface area of the effective specimen, and  $\sigma$  is the Stefan–Boltzmann constant.

Hemispherical total emissivity is computed for each data set on  $E$ ,  $I$ , and  $T_s$ . A final value for the hemispherical total emissivity of a specimen at a given temperature is then obtained by averaging the individual results at the plateau. Usually, the averaged range, indicated as B in Fig. 1, is less than the total plateau range indicated by A in the figure. The reasons for this are (a) not to include the initial portion of the plateau where the temperature is not yet completely stabilized and (b) not to include the later portion of the plateau where the contribution of the axial heat conduction in the effective specimen may become significant. These are discussed in more detail in Section 5.2.

### 3. MEASUREMENT SYSTEM

A schematic diagram of the measurement system used in this study is shown in Fig. 2. The measurement system, with the exception of the switch, the pyrometer, and the data acquisition system, is essentially the same as that described in earlier publications [1, 2]. The new items are discussed briefly below.

#### 3.1. Switch

The recently developed controllable solid-state switch consists of parallel connected 20 FETs with protective resistors. The specifications of the FET and the switch are listed in Table I. The switch is controlled by a control voltage (gate-source voltage), which is usually in the range from 0 to 10 V. In principle, current through an individual FET as well as the switch may be approximated by a quadratic function of the control voltage [7]:

$$I_{sw} = K_c (V_c - V_t)^2 \quad (V_c \geq V_t) \quad (2)$$

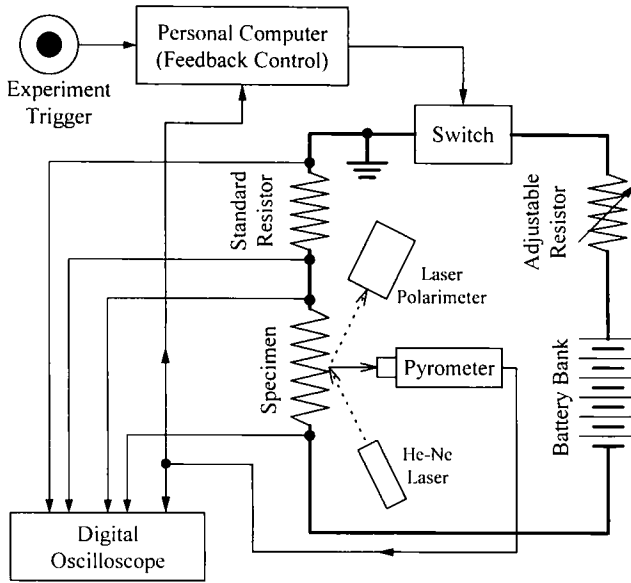


Fig. 2. Functional diagram of the measurement system that uses the feedback control technique.

where  $I_{sw}$  is the current through the switch,  $K_c$  is the gain of the current, which depends on the quantity and type of the FET which compose the switch,  $V_c$  is the control voltage, and  $V_t$  is the threshold voltage. Typical values of  $K_c$  and  $V_t$  for the switch used in the present measurements are listed in Table I.

Table I. Specifications of the Individual FET (n-type) and Overall Switch Used in the Present Measurements

	FET	Switch
Maximum continuous current	145 A	2900 A
Maximum voltage difference	100 V	100 V
Resistance	11 mΩ	1.8 mΩ
Maximum heat dissipation	500 W	10 kW
Response time (max.)	340 ns	340 ns
Control voltage ( $V_c$ ) <sup>a</sup>	0–20 V	0–20 V
Threshold voltage ( $V_t$ )	3.6 V	3.6 V
Gain ( $K_c$ )	27 A · V <sup>-2</sup>	530 A · V <sup>-2</sup>

<sup>a</sup> Switch is on for  $V_c = 10$  V; switch is off for  $V_c = 0$  V.

The maximum current capacity of the switch is limited by the maximum heat dissipation at the FET units. When the current is controlled continuously in accordance with Eq. (2), the heat dissipation at the FET units may become much larger than that in the simple on-and-off switching mode. In such a case, the current must be limited to a value lower than the maximum rating given in Table I in order to protect the FETs from being damaged.

### 3.2. Feedback Control

The proportional, integral, and differential (PID) feedback control theory is widely used in various types of feedback control systems. Based on this theory, the following is the basic equation which gives a control output [8]:

$$u = e + t_d \frac{de}{dt} + \frac{1}{t_i} \int e dt \quad (3)$$

where  $u$  is the normalized control output ( $-1 \leq u \leq 1$ ),  $t$  is time,  $t_d$  and  $t_i$  are the differential and integral constants, respectively, and  $e$  is the control error given by

$$e = (T_s - T_r)/T_p \quad (4)$$

where  $T_s$  is the set temperature,  $T_r$  is the measured radiance temperature of the specimen, and  $T_p$  is a constant which determines the sensitivity of the control system.

The normalized control output is related to the control voltage of the switch by

$$V_c = (u + 1)(V_{\max} - V_i)/2 + V_i \quad (5)$$

where  $V_{\max}$  is the maximum control voltage, which is approximately 10 V.

The stability and convergence of the controlled system are strongly dependent on the three constants,  $t_d$ ,  $t_i$ , and  $T_p$ , which are characteristic of each controlled system and operational condition. These constants were optimized before the measurements of hemispherical total emissivity through test experiments.

Another simplified control method is called the proportional and differential (PD) control method. This method uses only the first two terms in Eq. (3) (i.e.,  $t_i = \infty$ ). The advantages of the PD control method are the simplicity of the calculation and stability of the controlled system under

various operational conditions. On the other hand, as a disadvantage, a finite offset temperature from the set temperature which is subject to the change of heat balance within the specimen may appear even after the temperature has been well stabilized. However, the PD control method may be better for some applications where a fast time response is more important than a finite offset temperature as is in the present measurements of hemispherical total emissivity.

The feedback control was performed using a dedicated personal computer with A/D (analog-to-digital) and D/A (digital-to-analog) converters of 12-bit voltage precision. One cycle of the feedback control included the following steps.

- (a) An output voltage of the pyrometer is sampled by the A/D converter.
- (b) A radiance temperature is calculated from the output voltage.
- (c) A corresponding control voltage is computed using Eqs. (3), (4), and (5).
- (d) The control voltage is converted to a real voltage by the D/A converter.
- (e) The control voltage is transferred to the switch through a differential amplifier.

This cycle was repeated continuously during a feedback control experiment with a cycle time of approximately 0.7 ms.

### 3.3. Pyrometer

A high-speed optical pyrometer [9], operating at 651 nm (bandwidth, 20 nm), was used to measure the surface radiance temperature of the specimen. The target of the pyrometer was a circular area 0.2 mm in diameter. The range of temperature measurements was from approximately 1300 to 2000 K. Up to three neutral density filters were used to extend the measurements to temperatures above 2000 K.

The true temperature of the specimen was computed from the measured output voltage of the pyrometer using the following equation based on Planck's law:

$$T_{\text{true}} = \frac{c_2}{\lambda \log[1 + (\varepsilon_{n,\lambda} \tau K_v / V_p)]} \quad (6)$$

where  $T_{\text{true}}$  is the true temperature,  $c_2$  is the second of radiation constant (0.014388 m · K),  $\lambda$  is the effective wavelength,  $K_v$  is the characteristic

constant of the pyrometer,  $\varepsilon_{n,\lambda}$  is the normal spectral emissivity of the specimen surface,  $\tau$  is the total transmittance of the neutral-density filters, and  $V_p$  is the output voltage of the pyrometer. The pyrometer was calibrated against a secondary standard (tungsten-filament lamp), which, in turn, was calibrated by the Radiometric Physics Division at NIST. To account for the transmittance of the optical window of the experiment chamber, calibration of the pyrometer was performed including a window of the same material and thickness as the one used in the actual experiments. Transmittances of the three neutral density filters (0.515, 0.278, and 0.108) were determined by viewing the standard lamp alternately with and without a filter.

### 3.4. Data Acquisition

The output voltage of the pyrometer and the voltages across the standard resistor and the voltage probes were sampled and recorded every 0.2 ms with a 12-bit digital oscilloscope. After each experiment, these data were transferred to a personal computer and processed.

## 4. MEASUREMENTS

### 4.1. Specimens

Experiments were performed on a rod-shaped tantalum specimen having the following nominal dimensions: 1.6-mm diameter and 75-mm length. As reported by the manufacturer, the tantalum material was 99.9 + (mass%) pure, with the following major impurities (ppm): O, 61; W, 50; Ni, 32; Fe, 30; N, 20; C, 18; Al, Ca, Cr, Co, Cu, Mg, Mn, Mo, Nb, Si, Sn, Ti, V, and Zr, each 10 or less; and H, 5 or less. A pair of fine grooves, 25 mm apart, was fabricated at the middle portion of the specimen for the voltage probes. The surface of the specimen was polished with No. 4000 abrasive paper. Before the experiments, the specimen was preheated (250-ms pulse) to 2700 K five times in vacuum at about  $3 \times 10^{-4}$  Pa ( $2 \times 10^{-6}$  Torr). The experiments were conducted immediately after the preheating under the same vacuum level.

### 4.2. Normal Spectral Emissivity

Knowledge of the normal spectral emissivity,  $\varepsilon_{n,\lambda}$  of a specimen is necessary in order to determine its true temperature from the measured radiance temperature with an optical pyrometer. In the present study,  $\varepsilon_{n,\lambda}$  was measured simultaneously with the other experimental quantities with



a high-speed laser polarimeter described in detail elsewhere [10]. The measurements of  $\varepsilon_{n,\lambda}$  were at 633 nm, the wavelength of the helium–neon laser of the polarimeter. The measured values of  $\varepsilon_{n,\lambda}$  were converted to correspond to 651 nm, the pyrometer wavelength, by interpolating the earlier results [11] on  $\varepsilon_{n,\lambda}$  of tantalum (0.386 at 616 nm and 0.379 at 651 nm) measured at its melting point. This is a reasonable procedure since the difference in  $\varepsilon_{n,\lambda}$  between the two wavelengths (616 and 651 nm) is not large (1.8%) and  $\varepsilon_{n,\lambda}$  is a smooth function of temperature. According to this procedure, the difference in  $\varepsilon_{n,\lambda}$  of tantalum corresponding to 633 and 651 nm is about 0.9%, which corresponds to a temperature difference of about 3 K at 2800 K.

### 4.3. Hemispherical Total Emissivity

In a typical experiment for the determination of hemispherical total emissivity, the specimen was heated from room temperature to a preset high temperature in about 200 ms, then it was maintained at a constant temperature for about 500 ms utilizing the feedback control. This procedure was repeated several times, each time placing the preset temperature at a level higher than that in the previous experiment. This procedure yielded hemispherical total emissivity values at 11 temperatures over the range 2000 to 2800 K. This constituted the first series of measurements, which is referred to as Run 1. After Run 1, the procedure was repeated from the lowest to the highest temperature. This series of experiments is referred to as Run 2.

During each experiment, the following experimental quantities were measured: voltage drop across the effective specimen, current through the specimen, radiance temperature of the specimen, and normal spectral emissivity of the specimen. Hemispherical total emissivity for each point at the plateau were computed using Eq. (1) based on the room-temperature dimensions of the specimen. A single value for emissivity was obtained at the plateau by averaging the individual emissivity values over a finite period on the plateau (typically, about 200 ms).

Variations of radiance temperature, voltage, current, and power imparted to the specimen as functions of time in a typical experiment on tantalum are shown in Fig. 3. It can be seen that the power requirement at the temperature plateau is a small fraction (about 3%) of the power required during the rapid heating. Variation of the specimen radiance temperature at the plateau is shown on a sensitive scale in Fig. 4 for two feedback control modes. Random noise on the temperature is due mostly to the finite resolution of the A/D converter. It can be seen that in both the PD and the PID modes there are instabilities at the beginning of the plateau

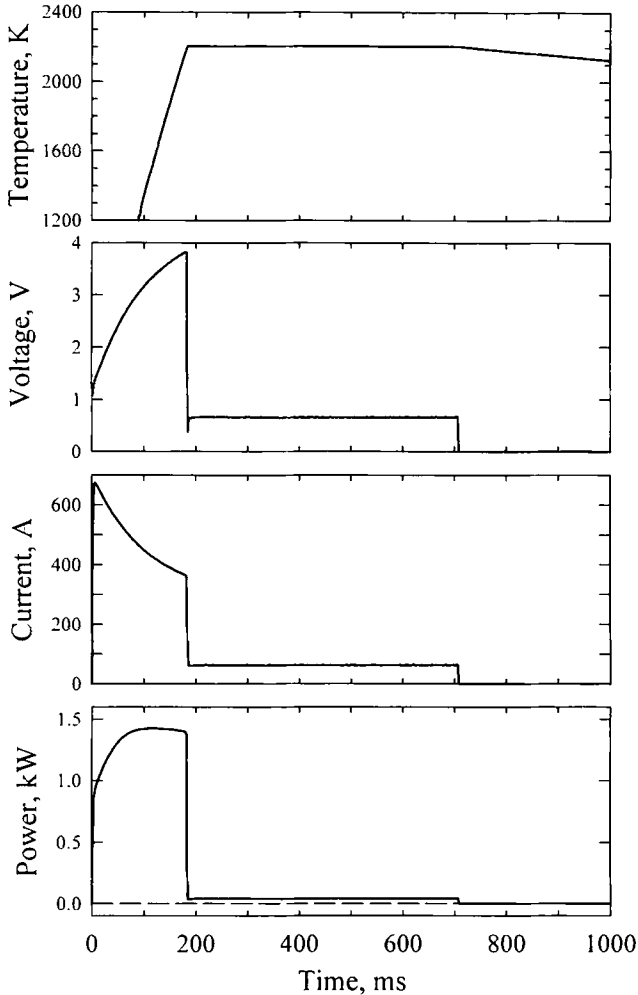


Fig. 3. Variations of the quantities, temperature, voltage, current, and power imparted to the specimen as a function of time in a typical experiment on a tantalum.

of about 1.2 and 0.5 K, respectively, which gradually taper off in both cases. This result demonstrates that the PD mode of operation is adequate provided that the beginning portion of the plateau is not considered in the computations. Thus, in all the experiments, the PD feedback control mode was used because of its advantages of having fast response time and good stability under different heating conditions.

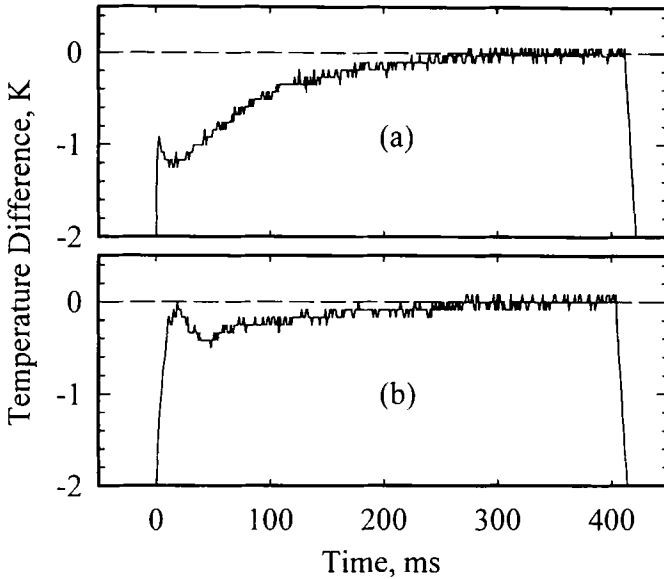


Fig. 4. Variation of the specimen temperature at the plateau for two feedback modes: (a) the simplified PD control mode and (b) the PID control mode. For both cases, temperature differences are given with respect to the temperature at the end of the plateau (approximately 2200 K).

## 5. RESULTS

### 5.1. Normal Spectral Emissivity

The results of measurements of the normal spectral emissivity of tantalum for the two runs are shown in Fig. 5. Each point represents the average of approximately 1000 measured emissivities at the plateau of an experiment. The standard deviation of the average is in the range 0.15–0.25%. The solid curve represents a quadratic function fitted (standard deviation = 0.20%) to the results of both runs using the least-mean squares method. The function for the normal spectral emissivity of tantalum at 633 nm in the temperature range 2000 to 2800 K is

$$\varepsilon_{n,\lambda} = 0.4526 - 3.399 \times 10^{-5}T + 3.260 \times 10^{-9}T^2 \quad (7)$$

where  $T$  is in K. The values of  $\varepsilon_{n,\lambda}$  at 100 K intervals, obtained from Eq. (7), are presented in Table II.

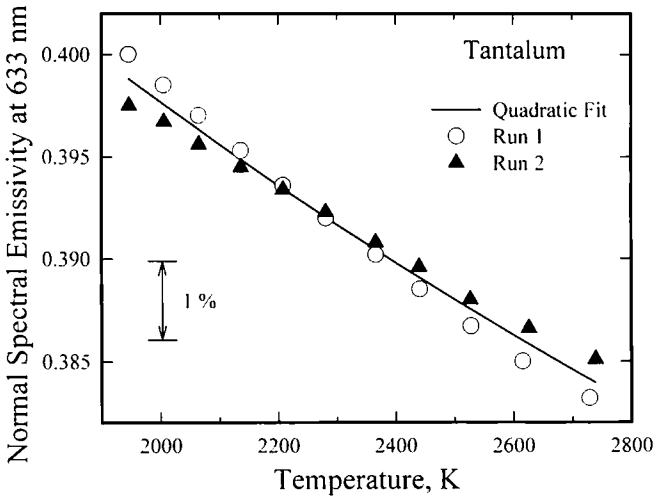


Fig. 5. Normal spectral emissivity of tantalum at 633 nm measured with the millisecond resolution laser-polarimeter. The solid curve represents a quadratic function [Eq. (7)] fitted to the entire data.

### 5.2. Hemispherical Total Emissivity

Figure 6 shows the results of the hemispherical total emissivity of the tantalum specimen obtained from the data at the plateau (2208 K) of a typical experiment. Fluctuations in emissivity are due largely to the fluctuations in current that result from the feedback control. The small overshoot in the emissivity values at the beginning of the plateau is likely to be due

Table II. Normal Spectral Emissivity and Hemispherical Total Emissivity of Tantalum Measured Using the Feedback Control Technique

Temperature (K)	Normal spectral emissivity at 633 nm	Hemispherical total emissivity
2000	0.398	0.228
2100	0.396	0.237
2200	0.394	0.247
2300	0.392	0.256
2400	0.390	0.265
2500	0.388	0.274
2600	0.386	0.282
2700	0.385	0.290
2800	0.383	0.298

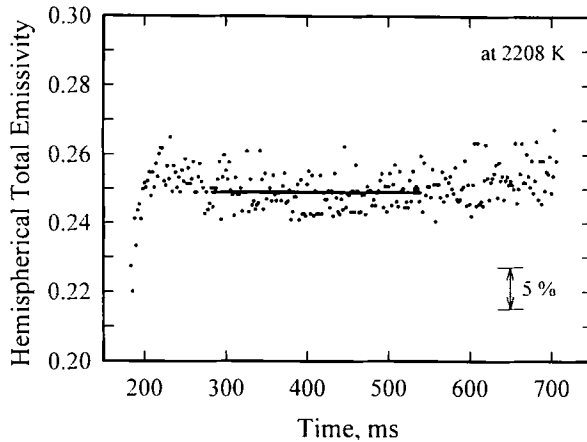


Fig. 6. Hemispherical total emissivity of tantalum in an experiment corresponding to a plateau temperature of 2208 K. A single emissivity value (0.248) was obtained by averaging the data over the range indicated by the line segment.

to instabilities in the specimen temperature. A gradual increase in the emissivity toward the end of the plateau may be due to the increased contributions of the axial heat conduction. For a given experiment, a single emissivity value is obtained by averaging (standard deviation = 1.9%) the measured emissivities over the plateau. The solid line in Fig. 6 shows the range of data used for the averaging.

The effect of heating rate on the measured emissivity of tantalum was investigated by performing several experiments on the tantalum specimen at different heating rates. The results of emissivity as a function of average heating rate at approximately 2200 K are shown in Fig. 7. Average heating rate is defined as  $(T_s - T_c)/t_s$ , where  $T_s$  and  $T_c$  are the plateau and the ambient temperatures, respectively, and  $t_s$  is the time required to heat the specimen from  $T_c$  to  $T_s$ . It can be seen that at low heating rates (less than  $10 \text{ K} \cdot \text{ms}^{-1}$ ), emissivity shows significant variations, while at high heating rates (greater than  $10 \text{ K} \cdot \text{ms}^{-1}$ ), emissivity converges to a constant value. The large deviations at the low heating rates may be attributed to the axial heat conduction from the boundaries of the effective specimen. All the subsequent experiments for emissivity measurements were conducted at heating rates greater than  $10 \text{ K} \cdot \text{ms}^{-1}$ .

The final results of hemispherical total emissivity as a function of temperature for all the experiments are shown in Fig. 8. The emissivity results for the two runs are in agreement within  $\pm 0.3\%$ . The solid curve represents a quadratic function fitted (standard deviation = 0.13%) to the

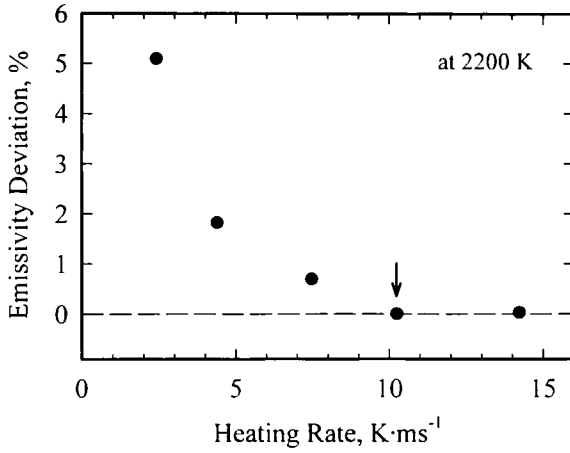


Fig. 7. Variation of hemispherical total emissivity as a function of average heating rate for tantalum at approximately 2200 K. The arrow indicates the lower limit of the average heating rate used in all the experiments conducted to obtain meaningful emissivity values.

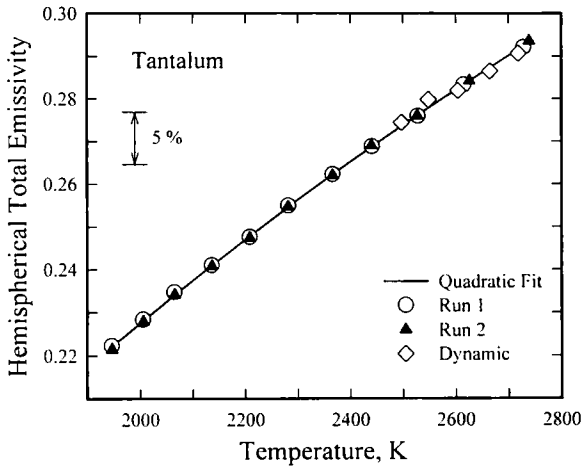


Fig. 8. Hemispherical total emissivity of tantalum measured using the feedback control technique. The solid curve represents a quadratic function [Eq. (8)] fitted to the data obtained by Runs 1 and 2. Representative data obtained by a dynamic technique are also shown.

results of both runs using the least-mean squares method. The function for the temperature range 2000 to 2800 K is

$$\varepsilon_{h,t} = -3.739 \times 10^{-2} + 1.644 \times 10^{-4}T - 1.598 \times 10^{-8}T^2 \quad (8)$$

where  $T$  is in K. The values of  $\varepsilon_{h,t}$  at 100 K intervals, obtained from Eq. (8), are presented in Table II.

In Fig. 8, results of hemispherical total emissivity obtained by a "dynamic" technique are also presented. The "dynamic" technique refers to the method used in the past in our laboratory [1] for measuring emissivity from data obtained during the radiative cooling period that followed the rapid pulse heating of the specimen. The agreement between the emissivity values obtained by the dynamic method and those by the new method presented in this paper is very good (within  $\pm 1\%$ ).

## 6. ESTIMATE OF UNCERTAINTIES

All uncertainties reported in this paper are based on the two-standard deviation level. Uncertainties due to individual major error sources were estimated on the basis of our experiences in the present measurements and in the earlier pulse-heating experiments in our laboratory [1, 10]. The resultant estimated total uncertainty in the measured hemispherical total emissivity was obtained by taking the square root of the sum of the squares of the individual uncertainties due to each error source.

Sources of uncertainties, their magnitudes, and their contributions to the uncertainty in hemispherical total emissivity evaluated at about 2400 K (midpoint of the temperature range of the present experiments) are presented in Table III. It may be seen that uncertainty in hemispherical total emissivity results from uncertainties in measured quantities and departure from assumed experimental conditions. Among the measured quantities, temperature is the dominant contributor to uncertainty. Uncertainty in temperature is due to uncertainties in measured radiance temperature (about 4 K) and normal spectral emissivity (less than 2%). Among the nonmeasured quantities, axial heat conduction in the effective specimen is the major source of uncertainty. Uncertainty due to axial heat conduction was estimated by considering the results of the investigation on emissivity deviations at various heating rates. Change in the temperature of the specimen at the plateau also causes an uncertainty because of the deviation from the steady-state condition. The temperature change was estimated from the time derivative of the temperature data at the plateau.

Fluctuations in current at the plateau period, which results from the feedback control, cause a relatively large (of the order of a few percent)

**Table III.** Sources of Uncertainties, Their Magnitudes, and Their Contributions to the Uncertainty in Hemispherical Total Emissivity Evaluated at About 2400 K<sup>a</sup>

Quantity	Uncertainty in quantity (%)	Contribution to uncertainty in emissivity (%)
Temperature	0.3 (7 K)	1.2
Current	0.2	0.2
Voltage	0.2	0.2
Specimen length	0.1	0.1
Specimen diameter	0.5	0.5
Current fluctuations	0.2	0.2
Axial heat conduction	1	1
Temperature change at plateau	0.05 (< 1 K)	0.5
Total uncertainty		1.8

<sup>a</sup> All uncertainties are based on the two-standard deviation level.

standard deviation (of an individual point) in emissivity. However, averaging the results at the plateau over about 1000 data points yields a standard deviation (of the mean) in emissivity data of about 0.2%.

The resultant total uncertainty in hemispherical total emissivity is estimated to be no more than  $\pm 2\%$ .

## 7. DISCUSSION AND CONCLUSION

Figure 9 shows the hemispherical total emissivity of tantalum reported in the literature [12–19]. The final fit to the present results, expressed by Eq. (8), is also shown by the solid curve. Since the optical properties of metallic surfaces are very sensitive to the surface conditions, such as surface roughness and contamination, the results given in the literature show a large scatter, over 20%. A portion of this scatter may be attributed to the consideration of the thermal expansion of the specimen; some of the data in the literature might have been corrected for expansion, while some others, including the present data, were not. However, the present results are in reasonably good agreement with most of the data reported in the literature in both the absolute value and the slope of the emissivity. The differences are almost within  $\pm 5\%$  if several data with large deviations are excluded.

The measurement method for hemispherical total emissivity using the feedback control technique is a new combined technique which utilizes advantages of both the steady-state and the transient methods, which have been traditionally considered to be exclusive of each other. Because of



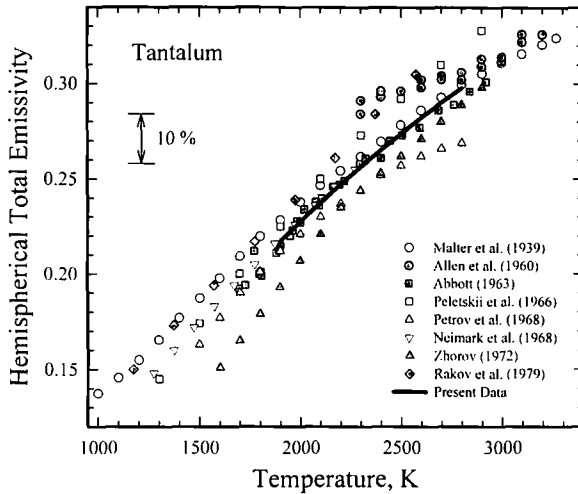


Fig. 9. Hemispherical total emissivity of tantalum reported in the literature [12–19].

the rapid heating to the high-temperature plateau, the problems due to the axial heat conduction in the effective specimen and contamination and oxidation of the specimen surface at high temperatures are, to a very large extent, avoided. Also, measurements under steady-state conditions do not require determination of heating and/or cooling rates and reduce random errors by averaging emissivity over a relatively long (200-ms) period.

**ACKNOWLEDGMENTS**

This work was supported in part by the Microgravity Science and Applications Division of NASA. Assistance provided by Dr. S. Krishnan of the Containerless Research Inc. in connection with the operation of the laser polarimeter is greatly appreciated.

**REFERENCES**

1. A. Cezairliyan, M. S. Morse, H. A. Berman, and C. W. Beckett, *J. Res. Natl. Bur. Stand. (U.S.)* **74A**:65 (1970).
2. A. Cezairliyan, *J. Res. Natl. Bur. Stand. (U.S.)* **75C**:7 (1971).
3. A. Cezairliyan, *Int. J. Thermophys.* **5**:177 (1984).
4. A. Cezairliyan, *Compendium of Thermophysical Property Measurement Methods, Vol. 2*, K. D. Maglič, A. Cezairliyan, and V. E. Peletsky, eds. (Plenum Press, New York, 1992), Chap. 17.
5. T. Matsumoto and A. Ono, *High Temp.- High Press.* **25**:525 (1993).
6. T. Matsumoto and A. Ono, *Int. J. Thermophys.* **16**:267 (1995).

7. P. Horowitz and W. Hill, *The Art of Electronics* (Cambridge University Press, Cambridge, 1989), Chap. 3.
8. K. J. Aström and T. Hägglund, *Automatic Tuning of PID Controllers* (Instrument Society of America, Research Triangle Park, NC, 1988), Chap. 2.
9. E. Kaschnitz and A. Cezairliyan, *Int. J. Thermophys.* **17**:1069 (1996).
10. A. Cezairliyan, S. Krishnan, and J. L. McClure, *Int. J. Thermophys.* **17**:1455 (1996).
11. A. Cezairliyan, J. L. McClure, and A. P. Müller, *High Temp.- High Press.* **25**:649 (1993).
12. L. Malter and D. B. Langmuir, *Phys. Rev.* **55**:743 (1939).
13. R. D. Allen, L. F. Glasier, Jr., and P. L. Jordan, *J. Appl. Phys.* **31**:1382 (1960).
14. G. L. Abbott, *U.S. Naval Rad. Def. Lab.* 1 (1963).
15. V. E. Peletskii and V. Yu. Voskresenskii, *High Temp.* **4**:329 (1966).
16. V. A. Petrov, V. Y. Chekhovskoi, and A. E. Sheindlin, *High Temp.* **6**:525 (1968).
17. B. E. Neimark and L. K. Voronin, *High Temp.* **6**:999 (1968).
18. G. A. Zhorov, *High Temp.* **10**:1202 (1972).
19. A. M. Rakov and B. A. Khrustalev, *Heat Transfer Sov. Res.* **11**:121 (1979).